NASA TECHNICAL MEMORANDUM

NASA TM X-71641

NASA TM X-71641

SODIUM SULFATE: VAPORIZATION THERMODYNAMICS AND ROLE IN CORROSIVE FLAMES

by Fred J. Kohl, Carl A. Stearns, and George C. Fryburg
Lewis Research Center
Cleveland, Ohio 44135

TECHNICAL PAPER to be presented at
International Symposium on Metal-Slag-Gas Reactions and Processes sponsored by the Electrochemical Society
Toronto, Canada, May 11-16, 1975

SODIUM SULFATE: VAPORIZATION THERMODYNAMICS AND ROLE IN CORROSIVE FLAMES

by Fred J. Kohl, Carl A. Stearns, and George C. Fryburg

National Aeronautics and Space Administration
Lewis Research Center
Cleveland, Ohio 44135

ABSTRACT

Gaseous species over liquid Na_2SO_4 have been identified by the technique of molecular beam mass spectrometry. The heat and entropy of vaporization of the Na_2SO_4 molecule have been measured directly as $\Delta H_{vap,1270K} = 273.6 \pm 12$ kJ $mole^{-1}$ (65.4 ± 2.9 kcal $mole^{-1}$) and $\Delta S_{vap,1270K} = 93.3 \pm 12$ J $mole^{-1}K^{-1}$ (22.3 ± 2.8 cal $mole^{-1}K^{-1}$). Comparisons of the experimental entropy with values calculated using various molecular parameters were used to estimate the molecular structure and vibrational frequencies for $Na_2SO_4(g)$.

The thermodynamic properties of gaseous and condensed phase Na_2SO_4, along with additional pertinent species, were used in a computer program to calculate equilibrium flame compositions and temperatures for representative turbine engine and burner rig flames. Compositions were calculated at various fuel-to-oxidant ratios with additions of sulfur to the fuel and the components of sea salt to the intake air. Temperatures for condensation of Na_2SO_4 were obtained as a function of sulfur and sea salt concentrations.

INTRODUCTION

The deposition of sodium sulfate from flames containing sodium and sulfur is regarded as one of the fundamental steps in the phenomenon of hot corrosion on turbine components. The presence of sulfur in fuels and the ingestion of various inorganic salts into combustion chambers along with intake air have been related to instances of hot corrosion attack in marine, industrial, and aircraft turbine engines. Because Na_2SO_4 is the major phase recovered from the turbine surfaces, it has been used extensively as a model compound for carrying out laboratory crucible- and furnace-type corrosion tests. An equilibrium thermodynamic description of the fate of sodium and sulfur and other elements leading to the formation of condensed Na_2SO_4 is useful in understanding the initial important stages of the corrosion mechanism.

It has been postulated (1) that gaseous Na_2SO_4 is formed in turbines by the reaction of oxidized sulfur with sodium chloride from sea salt:

$$2NaCl(g) + SO_2(g) + \tfrac{1}{2}O_2(g) + H_2O(g) = Na_2SO_4(g) + 2HCl(g) \quad (1)$$

$$2NaCl(g) + SO_3(g) + H_2O(g) = Na_2SO_4(g) + 2HCl(g) \quad (2)$$

Sodium sulfate itself is also a minor constituent in sea salt. Furthermore, for a complete description of the Na-S-O system, additional equilibria related to Na_2SO_4 (c)* vaporization must be considered: (a) molecular vaporization,

$$Na_2SO_4(c) = Na_2SO_4(g) \quad (3)$$

and (b) dissociative vaporization,

$$Na_2SO_4(c) = 2Na(g) + SO_2(g) + O_2(g) \quad (4)$$

$$Na_2SO_4(c) = Na_2O(c \text{ or } g) + SO_2(g) + \tfrac{1}{2}O_2(g) \quad (5)$$

$$= Na_2O(c \text{ or } g) + SO_3(g) \quad (5a)$$

$$Na_2SO_4(c) = 2NaO(g) + SO_3(g) \quad (6)$$

$$Na_2SO_4(c) + H_2O(g) = 2NaOH(c \text{ or } g) + SO_2(g) + \tfrac{1}{2}O_2(g) \quad (7)$$

The consideration of all of the above equilibria simultaneously at turbine temperatures and pressures, along with the major products of combustion, can lead to an understanding of the Na_2SO_4 deposition phenomenon.

All of the condensed phases and molecular species involved in the formation or vaporization of sodium sulfate are fairly well characterized thermodynamically except for the Na_2SO_4 molecule itself. Many separate determinations (2-9) of the "enthalpy of vaporization" (for reaction (3)) have been made ranging from 113 to 331 kJ $mole^{-1}$ (27 to 79 kcal $mole^{-1}$) with a corresponding entropy change of 29 to 251 J $mole^{-1}K^{-1}$ (7 to 60 cal $mole^{-1}K^{-1}$). Only the recent transpiration experiment results of Cubicciotti and Keneshea (2) and Fryxell et al. (3) show any agreement in the values of ΔH_{vap} and ΔS_{vap} for reaction (3) with the former finding $\Delta H_{vap,1550} = 296.6 \pm 8$ kJ $mole^{-1}$ (70.9 ± 1.8 kcal $mole^{-1}$), $\Delta S_{vap,1550} = 111.3 \pm 3$ J $mole^{-1}K^{-1}$ (26.6 ± 0.7 cal $mole^{-1}K^{-1}$) and the latter $\Delta H_{vap,1390} = 303.8 \pm 15$ kJ $mole^{-1}$

*Throughout this paper (c) refers to condensed state, either solid (s) or liquid (ℓ); (g) refers to gas.

(72.6±3.5 kcal $mole^{-1}$), $\Delta S_{vap,1390}$ = 115.5±10 J $mole^{-1}K^{-1}$ (27.6±2.5 cal $mole^{-1}K^{-1}$). The molecule has been observed directly only by Kosugi (4) in a mass spectrometer study where the ion current of $Na_2SO_4^+$ was recorded at four temperatures. Earlier an apparently thorough mass spectrometric investigation (5) failed to observe any $Na_2SO_4^+$. This discrepancy will be discussed later in this paper. The remaining experimenters assumed that Na_2SO_4 did exist as a molecular species and considered equations (3) and (4) to represent the most important reactions.

Several papers (1, 10-12) have dealt with the question of Na_2SO_4 deposition from turbine or burner rig flames, but all have suffered from the lack of consistent and reliable thermodynamic data for $Na_2SO_4(g)$. Therefore, the purpose of the present study is (1) to obtain complete and reliable thermodynamic data for the sodium sulfate vaporization/condensation process and (2) to demonstrate how these data can be employed to determine the conditions of Na_2SO_4 deposition in corrosive flame systems where the fuel and intake air are contaminated with sulfur and sea salt respectively. Because actual engine environment corrosion tests are prohibitively expensive and complicated, laboratory burner rigs are used to simulate the atmosphere and conditions of corrosive flames. With reliable thermodynamic data for all of the chemical species involved, the operating parameters necessary for realistic burner rig simulation of engine conditions can be specified.

Na_2SO_4 VAPORIZATION THERMODYNAMICS

Samples. Two sources of Na_2SO_4 were used for the mass spectrometric vaporization studies: (1) 99.999% Na_2SO_4, Apache Chemicals and (2) Certified ACS Na_2SO_4 (anhydrous), Fisher Scientific Co. Chloride analyses gave <1 ppm for the Apache and 6 ppm for the Fisher material. The pH of a 5% solution prepared according to the ACS Reagent Chemicals Specifications standard method was 6.96 and 7.05 respectively, indicating that no significant amount of acidic ($NaHSO_4$) or basic (NaOH, Na_2O) impurities were detected in either sample. Emission spectrographic analyses gave for the Apache and Fisher material respectively, 20 and 20 ppm Al, 250 and 400 ppm Ca, 40 and 40 ppm Fe, and 120 and 70 ppm Mg. X-ray powder diffraction patterns could be indexed as Na_2SO_4, form V, thenardite for the Apache material; and a mixture of Na_2SO_4, form V, and Na_2SO_4, form III with several extra lines for the Fisher material.

Experimental Apparatus. The double focusing mass spectrometer and high temperature Knudsen cell used in the present work have been described in detail previously (13). A schematic of the Knudsen cell oven assembly and ion source is given in Fig. 1. The cell is heated by radiation from tungsten filaments circumscribing the top and bottom and the temperatures are read by sighting into the cell blackbody holes through a window. Located between the Knudsen cell and ion source chamber

is a movable shutter slit which is used to interrupt or maximize the transmission of the molecular beam emanating from the orifice. Background pressure in the Knudsen cell region with the sample at temperature was usually in the 10^{-5} Nm^{-2} (10^{-7} torr) range.

Vapor Species Identification. The mass spectra of the vapors over $Na_2SO_4(\ell)$ were recorded at mass-to-charge ratios, m/e, up to about 600. In all cases, the observed ions were identified by mass-to-charge ratio and isotopic abundance. Typical mass spectra are given in Fig. 2.

Parent molecular species were identified by measurement of appearance potentials and ionization efficiency curves when ion intensities were sufficiently high. Measured values of the appearance potentials are listed in Table I. The values of the appearance potentials (A.P.) of O_2^+ and SO_2^+ agreed with the literature values (14) for the molecular ionization potential for O_2 and SO_2 respectively. The ionization potential of molecular SO is 12.1 eV, therefore SO^+ is a fragment ion in our mass spectra. Likewise the high value for the A.P. of Na_2O^+ indicates that it is a fragment when compared with the molecular A.P. of parent Na_2O of 5.5 eV(15). It is assumed that the other minor sulfur- and sodium-containing ions were also fragments except for SO_3^+ and $Na_2SO_4^+$. The value of 8.0 eV for the A.P. of $Na_2SO_4^+$ is quite reasonable for the parent molecular ion when compared with the values obtained for $K_2SO_4^+$, 7.4 eV, $Rb_2SO_4^+$, 8.6 eV, and $Cs_2SO_4^+$, 8.9 eV, by Ficalora et al. (5). Thus the only important parent molecular species were Na, O_2, SO_2, and Na_2SO_4.

To test for the possible interaction of molten Na_2SO_4 with various container materials, samples were heated in a number of different crucible materials for separate vaporization experiments: in platinum, with or without an Al_2O_3 liner; and in tungsten or tantalum, with a ZrO_2 liner. The spectra obtained from the platinum cell with or without the Al_2O_3 liner (Fig. 2a) were essentially identical and indicated that $Na_2SO_4^+$ was one of the three most intense ions along with Na^+ and $SO2+$. The identical and reproducible spectra plus the lack of any other observed species indicated that there was no reaction between the Pt or Al_2O_3 and the Na_2SO_4 under the conditions of the mass spectrometer experiments. The spectra obtained from the ZrO_2-lined tungsten or tantalum cells (Fig. 2b) showed a large increase in the Na^+ and SO_2^+ intensities relative to $Na_2SO_4^+$. In addition to the ions shown in Fig. 2b, $Na_2WO_3^+$, $Na_2WO_4^+$, $Na_2WO_5^+$, $Na_2WO_6^+$, and $Na_2W_2O_7^{+*}$ were observed in the case of the tungsten cell. These ions, along with Na^+, increased in relative intensity as a function of time at temperature while a decreasing intensity was recorded for $Na_2SO_4^+$. Visual examination of the

---

*Because of the possibility of overlapping spectra for $^{32}O_2$- and ^{32}S-containing ions, a S atom may be substituted for any two O atoms.

cells after experiments indicated that the molten Na_2SO_4 was able either to creep out or to penetrate the ZrO_2 liner and thus to come in contact and react with the tungsten or tantalum. Ficalora et al. (5) used Al_2O_3- or gold-lined tantalum cells for their vaporization studies on alkali sulfates and failed to identify $Na_2SO_4^+$. Their results may be explained on the basis of a reaction of the tantalum cell with the Na_2SO_4 leading to high SO_2 and Na pressures. In the present work, all of the subsequent measurements used to obtain thermodynamic data were carried out using the platinum cell without a liner.

Ion Intensity Measurements and Heats of Reactions. Because gaseous Na, O_2, SO_2, and Na_2SO_4 appear to be the only important vapor species in equilibrium with $Na_2SO_4(c)$ in vacuum, the mode of vaporization can be described completely, for all practical purposes, by reactions (3) and (4). For reaction (4), if $Na_2SO_4(\ell)$ is at unit activity, the equilibrium constant $K_4 = P_{Na}^2 P_{SO_2} P_{O_2}$, where P_i is the partial pressure of species i. For congruent vaporization of $Na_2SO_4(c)$ the number of moles of sodium vapor must be equal to twice the number of moles of SO_2 and O_2, ie. $n_{Na} = 2n_{SO_2} = 2n_{O_2}$; therefore, $P_{Na} = 2P_{SO_2} = 2P_{O_2}$. Thus the equilibrium constant can be rewritten as $K_4 = P_{Na}^4/4$. The ion intensity I_i is related to the pressure of species i by the simple relation $P_i = k_i I_i T$, where k_i is the mass spectrometer sensitivity constant and T is the absolute temperature; therefore, $K_4 = (k_{Na} I_{Na^+} T)^4/4$. From the van't Hoff equation, $d \ln K/d(1/T) = -\Delta H_T/R$, it follows that the least squares slope of a plot of log $(I_{Na^+}T)^4$ versus reciprocal temperature (1/T) is equal to $-\Delta H_T/R'$, where R' = (gas constant) (ln 10). Therefore to obtain the heat of reaction (4) it was necessary to measure the intensity of only one ion, Na^+, instead of three, Na^+, O_2^+, and SO_2^+, as a function of temperature. This was convenient because the non-condensible nature of O_2 and SO_2 resulted in only a partial shutter effect for these two species (about 30% and 95% respectively) which would have limited the accuracy of the determination of their intensities. The intensity of Na^+ was measured at 27 temperatures over the range 1192-1411 K. See Fig. 3. The experimental value of $\Delta H_{1300} = 1229 \pm 42$ kJ mole^{-1} (293.8 ± 10 kcal mole^{-1}) is in excellent agreement with the calculated value of 1215 kJ mole^{-1} (290.5 kcal mole^{-1}) based on JANAF data (16) for $Na_2SO_4(c)$, $Na(g)$, $O_2(g)$, and $SO_2(g)$.

To determine the heat of reaction (3), $I_{Na_2SO_4^+}$ was measured as a function of temperature. The results of two experiments are plotted in Fig. 4. Exp. I used Apache Na_2SO_4 while the Fisher material was used in Exp. II. The values of $I_{Na_2SO_4^+}$ at a given temperature are different in Exp. I and Exp. II because of differences in spectrometer settings and crucible alignment and are not due to any real difference in the samples. The ΔH values for the two experiments can be averaged to yield $\Delta H^\circ_{vap,1270} = 273.6 \pm 12$ kJ mole^{-1} (65.4 ± 2.9 kcal mole^{-1}).

Vapor Pressures and Entropy of Vaporization. In order to calculate vapor pressures for Na_2SO_4, the mass spectrometer sensitivity constant k (corresponding to the experimental conditions employed in Exp. I) from

the relation $P_i = k_i I_i T$ was obtained by the well-documented silver calibration method (13). The $I_{Na_2SO_4^+}$ values measured in Exp. I were converted to pressures and fit by the method of least squares to give

$$\log P_{Na_2SO_4} = \frac{-14,440}{T(K)} + 4.874(atm) = \frac{-14,440}{T(K)} + 9.880 \ (Nm^{-2})$$
$$(1196 - 1349 \ K).$$

For reaction (3), the entropy of vaporization ΔS_{vap} is related to the intercept of a plot of log $P_{Na_2SO_4}$ versus 1/T by the relation

$$\log P_{Na_2SO_4}(atm) = \frac{-\Delta H}{R'}\left(\frac{1}{T}\right) + \frac{\Delta S}{R'}.$$

Therefore $\Delta S_{vap,1267} = 93.3 \pm 12$ J mole^{-1}K^{-1} (22.3 ± 2.8 cal mole^{-1}K^{-1}). The estimated error in ΔS is based on an uncertainty of a factor of 4 in the values of the Na_2SO_4 pressures. The results are plotted in Fig. 5. If $\Delta S_{vap,1267}$ is combined with the absolute entropy of $Na_2SO_4(\ell)$ at 1267 K, 439.3 J mole^{-1}K^{-1} (105.0 cal mole^{-1}K^{-1}) (16), the absolute entropy of gaseous Na_2SO_4 is obtained as $S_{1267} = 532.6$ J mole^{-1}K^{-1} (127.3 cal mole^{-1}K^{-1}).

Molecular Structure and Thermodynamic Functions. It is necessary to generate a complete table of thermodynamic functions for a substance if calculations are to be made at temperatures outside of the range of the experimental determination of the thermodynamic properties. The methods of statistical mechanics which are used to generate such a table for a gaseous molecule require that the molecular geometry and other constants be specified. Because the molecular constants for the Na_2SO_4 molecule have not been determined experimentally, it was necessary to estimate these parameters. The structure selected had D_{2d} ($\sigma = 4$) symmetry based on the similar symmetry assigned to Cs_2SO_4 by Belyaeva et al. (17) on the basis of an IR spectroscopic study. The molecule can be pictured as having a central sulfur atom surrounded at the corners of a tetrahedron by four oxygen atoms with bridging sodium atoms between 2 pairs of oxygens. The internuclear distances chosen were 1.60×10^{-10}m for S-O and 2.04×10^{-10}m for Na-O. The product of the moments of inertia was calculated as $77,800 \cdot 10^{-117}$ gm^{3}cm^6. Cubicciotti and Keneshea (2) have also estimated the structure and molecular constants for Na_2SO_4 but chose a lower symmetry C_{2v} structure based on an older determination of the structure of Cs_2SO_4 (18).

A non-linear polyatomic molecule with seven atoms has 15 fundamental vibrational frequencies. For Na_2SO_4 nine of these can be assigned to the sulfate core. These nine are given values identical to those found in crystalline sulfates: 980, 450(2), 1100(3), and 620(3) cm^{-1} (19). The remaining six frequencies were assigned by comparison of the

frequencies for other sulfates (H_2SO_4, D_2SO_4, Cs_2SO_4) (16,17) and a comparison of the calculated and experimental values of the absolute entropy of Na_2SO_4. An initial estimate of these frequencies was made as 1500(2), 200(2) and 100(2) cm^{-1} (20). The absolute entropy at 1267 K was calculated and compared with the experimental value; the values of the frequencies were then revised and another comparison made until the calculated and experimental values agreed within 0.21 J $mole^{-1}K^{-1}$ (0.05 cal $mole^{-1}K^{-1}$). The final values obtained were 1000(2), 150, 140, and 90(2) cm^{-1}. The thermodynamic functions given in Table II were calculated by use of a NASA computer program (21) with the rigid rotator-harmonic oscillator approximation.

Summary and Comparison of Thermodynamic Data. The experimental values for the heat of molecular vaporization, reaction (3), from Exp. I and II at 1267 and 1273 K respectively were combined with heat contents for $Na_2SO_4(g)$ and $Na_2SO_4(c)$ and averaged to yield $\Delta H^\circ_{vap,298}$ = 351.9 kJ $mole^{-1}$ (84.1 kcal $mole^{-1}$). This value was combined with the standard heat of formation of Na_2SO_4 (form V,298) = -1387 kJ $mole^{-1}$ (-331.6 kcal $mole^{-1}$) (16) to yield the standard heat of formation of -1036 kJ $mole^{-1}$ (-247.5 kcal $mole^{-1}$) for $Na_2SO_4(g)$. The heat of formation was used along with the molecular parameters estimated for Na_2SO_4 to calculate the vapor pressure of Na_2SO_4 over the wide temperature range shown in Fig. 5. This final extrapolated line passes slightly above the pressures derived in Exp. I because the heat of vaporization was obtained as an average of the values from Exps. I and II. The vapor pressure data of Liander and Olsson (8), Kroger and Stratmann (7), Cubicciotti and Keneshea (2), and Fryxell et al. (3) are also plotted in Fig. 5. It is apparent that there is good agreement between the values obtained by Cubicciotti and Keneshea and Fryxell et al. with the present data.

ROLE OF Na_2SO_4 IN FLAMES

Computer Program. The widely used NASA computer program employed here to calculate complex chemical equilibrium compositions and thermodynamic mixture properties has been described in detail previously (22). This program is based on the minimization of free energy approach to chemical equilibrium calculations subject to the constraints of maintaining a proper mass balance between reactants and products. The program permits the calculation of chemical equilibrium composition for heterogeneous systems for assigned thermodynamic states such as temperature-pressure (T,P) and enthalpy-pressure (H,P). For the present work, the role of Na_2SO_4(c or g) in typical turbine engine or burner rig combustion systems was examined by obtaining results describing flame temperatures and compositions as a function of fuel-to-oxidant ratio, with additions of sulfur to the fuel and of the components of sea salt to the intake air.

Program Input. The fuel used in most aircraft turbine engines and laboratory burner rigs and for all calculations made here was ASTM JET A-1 (23) with the empirical formula $CH_{1.9185}(\ell)$ and an assigned enthalpy at 298 K of -22.2 kJ $mole^{-1}$ (-5300 cal $mole^{-1}$). The ASTM aviation turbine fuel standard specifications limit the maximum total weight percent of sulfur in this fuel to 0.3%. In practice, 0.05% sulfur is a typical value encountered for the everyday use of this fuel. Sulfur is present in petroleum mainly as organic compounds such as mercaptans, aliphatic and aromatic sulfides and disulfides, cyclic compounds, thiophene, and polysulfides. It may also appear as H_2S and even elemental sulfur. For calculational purposes, sulfur was added to the fuel in its elemental state over a range of 0.0 to 0.3 weight percent.

The oxidant used for all calculations was air with the empirical formula $N_{1.56176}O_{0.41959}Ar_{0.009324}C_{0.000300}(g)$ and an assigned enthalpy of -118 J $mole^{-1}$ (-28.2 cal $mole^{-1}$) at 298 K. For burner rig type calculations, one weight percent $H_2O(g)$ was added to approximate 50% relative humidity at 298 K. The composition of sea salt was taken as a combination of the five most important inorganic salts which make up ASTM Standard substitute ocean water (24): in wt. %, NaCl, 68.78, $MgCl_2$, 14.57, Na_2SO_4, 11.46, $CaCl_2$, 3.25, and KCl, 1.93. Taken together, these salts make up 99.1% of the salts used to make substitute ocean water. Total sea salt concentrations of 0.1 to 20 ppm by weight in the oxidant were used in the calculations.

Although the program can carry out constant pressure combustion calculations at any reasonable pressure and combustor inlet air temperature, specific values were chosen here to represent "typical" conditions for a modern aircraft turbine engine and atmospheric burner rig. For the turbine engine the combustion pressure was taken as 2.24×10^6 Nm^{-2} (22.1 atm, 325 PSIA) with an inlet temperature of 811 K (1000°F); for the one atmospheric pressure burner rig, a temperature of 298 K was taken as the inlet temperature. Fuel inlet temperatures were taken as 298 K for both cases.

Flame Temperatures and Compositions. The computer program was operated in the H,P mode with the initial and final enthalpies equal to that of the reactants at the inlet temperatures to calculate the equilibrium adiabatic flame temperatures. Flame temperatures as a function of fuel/oxidant mass ratio are shown in Fig. 6. The temperatures for the turbine engine flame, which correspond ideally to combustor exit or turbine inlet temperatures, vary over the range of 1075 to 1800 K for the case of the typical aircraft turbine with a peak at approximately 2600 K for a stoichiometric fuel/oxidant ratio. The one atmosphere burner rig flame is somewhat hotter over the normal operating range varying from 1225 to 1950 K and peaking at about 2260 K for near stoichiometric operation.

The chemical equilibrium compositions of the reacted flame gases at the adiabatic flame temperatures are given in Figs. 7 and 8 as a function of fuel/oxidant mass ratio for the two combustion systems considered here. The species shown are those which were present at a mole fraction of greater than 10^{-10} for a significant range of fuel/oxidant ratios for each case. To arrive at the distribution of molecular species depicted in Figs. 7 and 8 the program considered over 150 gaseous and condensed species made up of CHNOSCl combinations and Na-, Mg-, Ca-, and K-CHNOSCl combinations. A list of the species considered is given in Table III. The thermodynamic data for most of these species was obtained from the JANAF tables (16). It must be pointed out that only those molecular species for which the program was given thermodynamic data were considered in the calculations. Although thermodynamic data for some chemically stable gaseous and condensed species have not been included for the present calculations, ie. notably K_2SO_4(c or g), $CaSO_4$(c or g), $MgSO_4$(c or g), $Ca(OH)_2$(g), Na_2S(c or g), Na_2CO_3(c or g), their inclusion at a future time is not expected to significantly perturb the present Na_2SO_4 results because of their relative stabilities and the fact the levels of the Mg-, Ca- and K-salts are quite low in sea salt compared with sodium.

The composition results show that, as expected, the major gaseous products for both flames are N_2, O_2, CO_2, H_2O, Ar, NO, OH, and CO with a large number of CHNOS species at lower levels. Chlorine appears mainly as HCl while the sodium is distributed in a complex pattern between Na_2SO_4(c), NaCl(g), NaOH(g), Na_2SO_4(g), and Na(g). At low values of the fuel/oxidant mass ratio (corresponding to low flame temperatures) and up to a sharp cut off point, the sodium is tied up almost exclusively as Na_2SO_4(c). Under these conditions the partial vapor pressure of Na_2SO_4(g) equals its equilibrium value, which defines the condition for the onset of condensation. Gaseous Na_2SO_4 is present in significant amounts over a relatively narrow fuel/oxidant ratio range and is always present at a molar concentration of less than 10% of NaCl(g). At high fuel/oxidant ratios, NaOH(g) and Na(g) account for most of the sodium. The magnesium, calcium, and potassium are present mainly as condensed phase oxides and halides at low temperatures and gaseous hydroxides or oxides at higher temperatures.

The major conclusions to be drawn from the flame composition calculations are that: 1) Na_2SO_4 can be formed in the flame as a condensed phase and/or a gas; 2) that its formation is strongly dependent on the temperature of the flame as determined by the fuel/oxidant ratio; and 3) that over <u>most</u> of the range of flame temperatures, NaCl, NaOH, or Na are the major Na-containing species.

<u>Conditions for Na_2SO_4 Condensation</u>. The major question with regard to Na_2SO_4 deposition as related to the phenomenon of hot corrosion of turbine components is "under exactly what conditions can Na_2SO_4(c) be deposited?" In the previous section we have pointed out that the existence of Na_2SO_4(c or g) in flames is strongly dependant on a number of

identifiable variables: fraction of sulfur in fuel, concentration of sea salt in oxidant, fuel/oxidant ratio, temperature, and pressure. It was shown that $Na_2SO_4(g)$ could condense even at some flame temperatures under certain conditions in both engine and rig type flames. Referring back to Figs. 7 and 8 it can be seen that for engines, the possibility of condensation in the flame exists in the normal idle range and at the low end of the takeoff and cruise ranges. If condensed Na_2SO_4 already exists at the combustor exit conditions, deposition and additional condensation will surely take place further downstream in the drive turbine section where both gas temperatures and component surface temperatures are considerably below the gas turbine inlet temperature. However, for the burner rig flame, condensation will occur in the flame itself only at fuel/oxidant ratios normally below the normal operating range. Thus a second question regarding sodium sulfate deposition arises, "under what conditions can the sodium sulfate be made to condense from a burner rig flame?" In a burner rig experiment, the sample surface temperature and gas temperature in the vicinity of the specimens are usually also considerably lower than that of the combustor exit temperature. If the vapor pressure of $Na_2SO_4(g)$ in the gas comprising the boundary layer surrounding a test specimen equals the equilibrium vapor pressure at the boundary layer temperature, condensation can begin.

In order to precisely determine condensation temperatures for Na_2SO_4 under various conditions, the computer program was run in the T,P mode with variable amounts of sulfur, sea salt, and variable fuel/oxidant ratios for the turbine engine and burner rig flames. Runs were made with different temperatures until the temperature below which Na_2SO_4 would condense was determined with a precision of ±1 K. The results are plotted in Figs. 9 and 10 for various sea salt concentrations as condensation temperature versus the weight fraction of sulfur in the fuel multiplied by the fuel/oxidant mass ratio. Consideration of only the weight fraction of sulfur in the fuel without specifying the fuel/oxidant ratio is insufficient because the <u>total</u> amount of sulfur reacting with a given amount of sea salt is needed to characterize the system. For a given sea salt concentration the condensation temperature can vary by approximately 140 K for the turbine engine and 110 K for the burner rig. The difference of combustor pressures between the engine and the rig in the examples given dictates that in order to obtain a condensation temperature in a rig as high as that in an engine requires approximately 100 times as much salt for a given amount of sulfur. From the results of calculations made with sulfur and sea salt concentrations other than those used for the two detailed examples (Figs. 7 and 8), it is apparent that the amounts of sodium sulfate and the distribution of sodium among other species in flames is strongly dependent on input levels (particularly for the sea salt concentration and less so for the sulfur) along with the fuel/oxidant ratio. Neither factor should be overlooked in a general description of the fate of the sodium and sulfur in flames.

Figs. 9 and 10 show that for a given fuel/oxidant ratio, the condensation temperature varies strongly as a function of sulfur content at low sulfur percentages but is practically independent at high percentages. Several investigators (25-28) have evaluated experimentally the effects of sulfur level on deposition of Na_2SO_4 on burner rig specimens by measurement of either the amount of material condensed or the degree of corrosion. Their results, on the whole, agree with the behavior indicated by Fig. 10.

Condensation can just begin at the calculated condensation temperatures given in Figs. 9 and 10. As the gas temperature drops below the condensation temperature the distribution of Na_2SO_4 between the gaseous and condensed states will change until at some lower temperature essentially all of the Na_2SO_4 is condensed. The fraction of Na_2SO_4 condensed is plotted as a function of temperature for both flame types in Figs. 11 and 12 for specified fuel/oxidant ratio and sulfur levels. For the engine flame 95% of the Na_2SO_4 condenses within about 75 K of the onset of condensation while for the burner rig 95% condenses within 65 K.

CONCLUDING REMARKS

In summary, we have experimentally verified the existence of $Na_2SO_4(g)$ and determined its thermodynamic properties. We have demonstrated that an equilibrium thermodynamic description of the fate of sodium and sulfur and other elements leading to the formation of condensed Na_2SO_4 is useful in understanding the behavior of Na_2SO_4 in corrosive flames.

Further work is needed along the lines of trying to establish the amount of $Na_2SO_4(c)$ that is deposited as a function of time under given temperatures, sulfur, and salt concentrations so that the amounts of salt in furnace corrosion tests can be related to an actual engine or rig case. In addition it remains for an experimental verification of thermodynamic equilibrium to be demonstrated by kinetic studies of the various Na_2SO_4-forming flame reactions.

ACKNOWLEDGMENTS

The authors wish to thank Gilbert Santoro and Bonnie McBride of NASA and Michael Zehe of Case Western Reserve University for enlightening discussions.

REFERENCES

1. M. A. DeCrescente and N. S. Bornstein, Corrosion, 24, 127 (1968).
2. D. Cubicciotti and F. J. Keneshea, High Temp. Sci., 4, 32 (1972).
3. R. E. Fryxell, C. A. Trythall, and R. J. Perkins, Corrosion, 29, 423 (1973).
4. T. Kosugi, Kogyo Kagaku Zasshi, 73, 1087 (1970).
5. P. J. Ficalora, O. M. Uy, D. W. Muenow, and J. L. Margrave, J., Amer. Ceram. Soc., 51, 574 (1968).
6. D. G. Powell and P. A. H. Wyatt, J. Chem. Soc., (A), 3614 and references therein (1971).
7. C. Kröger and J. Stratmann, Glastechn. Ber., 34, 311 (1961).
8. H. Liander and G. Olsson, IVA-Tidskrift for Teknisk Vetenskaplig Forskring 4, 145 (1937).
9. A. F. Fotiev and B. V. Slobodin, Russ. J. Inorg. Chem., 10, 309 (1965).
10. J. G. Tschinkel, Corrosion, 28, 161 (1972).
11. W. D. Halstead, in "Deposition and Corrosion in Gas Turbines," Ed. by A. B. Hart and A. J. B. Cutler, p. 22, John Wiley & Sons (1973).
12. J. F. G. Condé, in "High Temperature Corrosion of Aerospace Alloys," AGARD-CP-120, 1972, pp. 203-220.
13. C. A. Stearns and F. J. Kohl, NASA TN D-7613 (1974).
14. R. W. Kiser, "Introduction to Mass Spectrometry and Its Applications," Prentice-Hall, 1965, Appendix IV, pp. 301-320.
15. D. L. Hildenbrand and E. Murad, J. Chem. Phys., 53, 3403 (1970).
16. D. R. Stull, ed., "JANAF Thermochemical Tables," Dow Chemical Co.
17. A. A. Belyaeva, M. I. Dvorkin, and L. D. Shcherba, Optics and Spect. (Russ.) 31, 309 (1971).
18. A. N. Spiridonov, A. N. Khodchenkov, and P. A. Akishin, J. Struct. Chem. (USSR), 6, 601 (1965).
19. K. Nakamoto, "Infrared Spectra of Inorganic and Coordination Compounds," John Wiley & Sons (1963).
20. Michael Zehe, Cas Western Reserve University, private communication.
21. B. J. McBride and S. Gordon, NASA TN D-4097 (1967).
22. S. Gordon and B. J. McBride, NASA SP-273 (1971).
23. Aviation Turbine Fuels, ASTM Spec. D1655-73, 1973.

24. Substitute Ocean Water, ASTM Spec. D1141-52, 1971.

25. R. M. Schirmer and H. T. Quigg, "Effect of Very Low Sulfur in JP-5 Fuel on Hot Corrosion," Phillips Petroleum Co., May 1971, AD-725619.

26. H. L. Wheaton, "Study of the Hot Corrosion of Superalloys," Avco Lycoming Division, Rept. No. 2195.8.2, 1966.

27. P. A. Bergman, "Saline Corrosion of Aircraft Gas Turbine Materials at Temperatures up to 2000 F," General Electric Corp. Rept. R64SE10, 1964.

28. F. Greenwood and L. Fiedler, "Oxidation-Corrosion Testing of Coated and Uncoated Gas Turbine Alloys," Boeing Co. Rept. TR-1086, 1963.

TABLE I. - APPEARANCE POTENTIALS AND PARENT SPECIES

Ion	Appearance Potential (eV)	Parent Species
$^{23}Na^+$	5.14 (Standard, ref. 14)	Na
$^{32}S^+$	- -	SO_2
$^{32}O_2^+$	12.1±0.3 (12.07, ref. 14)	O_2
$^{39}NaO^+$	- -	Na_2SO_4
$^{48}SO^+$	15.7±0.5 (12.1 from SO, ref. 14)	SO_2
$^{62}Na_2O^+$	9.3±1.0 (5.5 from Na_2O, ref. 15)	Na_2SO_4
$^{64}SO_2^+$	12.2±0.3 (12.34, ref. 14)	SO_2
$^{78}Na_2O_2^+$	- -	Na_2SO_4
$^{80}SO_3^+$	- -	SO_3
$^{96}SO_4^+$	- -	Na_2SO_4
$^{126}Na_2SO_3^+$	- -	Na_2SO_4
$^{142}Na_2SO_4^+$	8.0±0.5	Na_2SO_4

TABLE II.- THERMODYNAMIC FUNCTIONS FOR $Na_2SO_4(g)$

Temperature, T, K	Heat capacity, C_p°, J mole^{-1}K^{-1}	Heat content, $H_T^\circ - H_0^\circ$, kJ mole^{-1}	Entropy, S_T°, JK^{-1} mole^{-1}	Free-energy function, $-(G_T^\circ - H_0^\circ)/T$, JK^{-1} mole^{-1}	Log Kp[a]
298.15	97.74	20.35	344.17	275.91	401.95
300	98.07	20.54	344.78	276.33	399.22
400	113.4	31.14	375.19	297.33	289.20
500	124.6	43.07	401.77	315.62	223.09
600	132.5	55.95	425.22	331.97	178.97
700	138.1	69.49	446.08	346.81	147.43
800	142.1	83.51	464.80	360.41	123.77
900	145.0	97.87	481.71	372.96	105.36
1000	147.3	112.49	497.11	384.62	90.64
1100	149.0	127.31	511.23	395.50	78.59
1200	150.3	142.28	524.26	405.69	68.55
1300	151.4	157.36	536.33	415.28	60.06
1400	152.3	172.55	547.58	424.33	52.78
1500	153.0	187.81	558.11	432.91	46.47
1600	153.5	203.14	568.00	441.04	40.95
1700	154.0	218.52	577.33	448.79	36.09
1800	154.4	233.94	586.14	456.18	31.76
1900	154.8	249.40	594.50	463.24	27.89
2000	155.1	264.90	602.45	470.00	24.42
2100	155.4	280.42	610.03	476.49	21.27
2200	155.6	295.97	617.26	482.73	18.41
2300	155.8	311.54	624.18	488.75	15.80
2400	156.0	327.13	630.81	494.51	13.40
2500	156.1	342.73	637.18	500.09	11.20
2600	156.3	358.35	643.31	505.48	9.17
2700	156.4	373.98	649.21	510.70	7.30
2800	156.5	389.62	654.90	515.75	5.55
2900	156.6	405.28	660.39	520.64	3.93
3000	156.7	420.94	665.70	525.39	2.41

[a]Reference state for calculating Log Kp: gaseous O_2, solid Na from 298.15 to 371 K, liquid Na from 371 to 3000 K, solid crystal S from 298.15 to 388, liquid S from 388 to 2000, gaseous S from 2000 to 3000.

TABLE III.- SPECIES CONSIDERED IN COMPUTER CALCULATIONS
[Phases listed without parentheses are gases]

Ar	C(s)	C	CCl	CCl_2	CCl_3
CCl_4	CH	CH_2	CH_2O	CH_3	CH_4
CN	CN_2	CO	COCl	$COCl_2$	COS
CO_2	CS	CS_2	C_2	C_2Cl_2	C_2H
C_2H_2	C_2H_4	C_2H_6	C_2N	C_2N_2	C_2O
C_3	C_3O_2	C_4	C_5	Ca(s)	Ca(ℓ)	Ca
CaCl	$CaCl_2$(s)	$CaCl_2$(ℓ)	$CaCl_2$	CaO(s)	CaO(ℓ)
CaO	CaOH	$Ca(OH)_2$(s)	CaS(s)	Cl	ClCN
ClO	ClO_2	Cl_2	Cl_2O	H	HCl
HCN	HCO	HNCO	HNO	HNO_2	HNO_3
HO_2	H_2	H_2O(s)	H_2O(ℓ)	H_2O	H_2O_2
H_2S	H_2SO_4(ℓ)	H_2SO_4	K(S)	K(ℓ)	K
KCl(s)	KCl(ℓ)	KCl	KO	KOH(s)	KOH(ℓ)
KOH	K_2	K_2O(s)	$(KOH)_2$	Mg(s)	Mg(ℓ)
Mg	MgCl	$MgCl_2$(s)	$MgCl_2$(ℓ)	$MgCl_2$	MgH
MgN	MgO(s)	MgO(ℓ)	MgO	MgOH	$Mg(OH)_2$
MgS(s)	MgS	N	NCO	NH	NH_2
NH_3	NO	NOCl	NO_2	NO_2Cl	NO_3
N_2	N_2H_4	N_2O	N_2O_4	N_2O_5	N_3
Na(s)	Na(ℓ)	Na	NaCl(s)	NaCl(ℓ)	NaCl
NaCN	NaH	NaO	NaOH(s)	NaOH(ℓ)	NaOH
Na_2	$(NaCl)_2$	Na_2O(s)	Na_2O(ℓ)	Na_2O	$(NaOH)_2$
$(NaCN)_2$	Na_2SO_4(s)	Na_2SO_4(ℓ)	Na_2SO_4	O	OH
O_2	O_3	S(s)	S(ℓ)	S	SH
SN	SO	SO_2	SO_2Cl_2	SO_3	S_2
S_8					

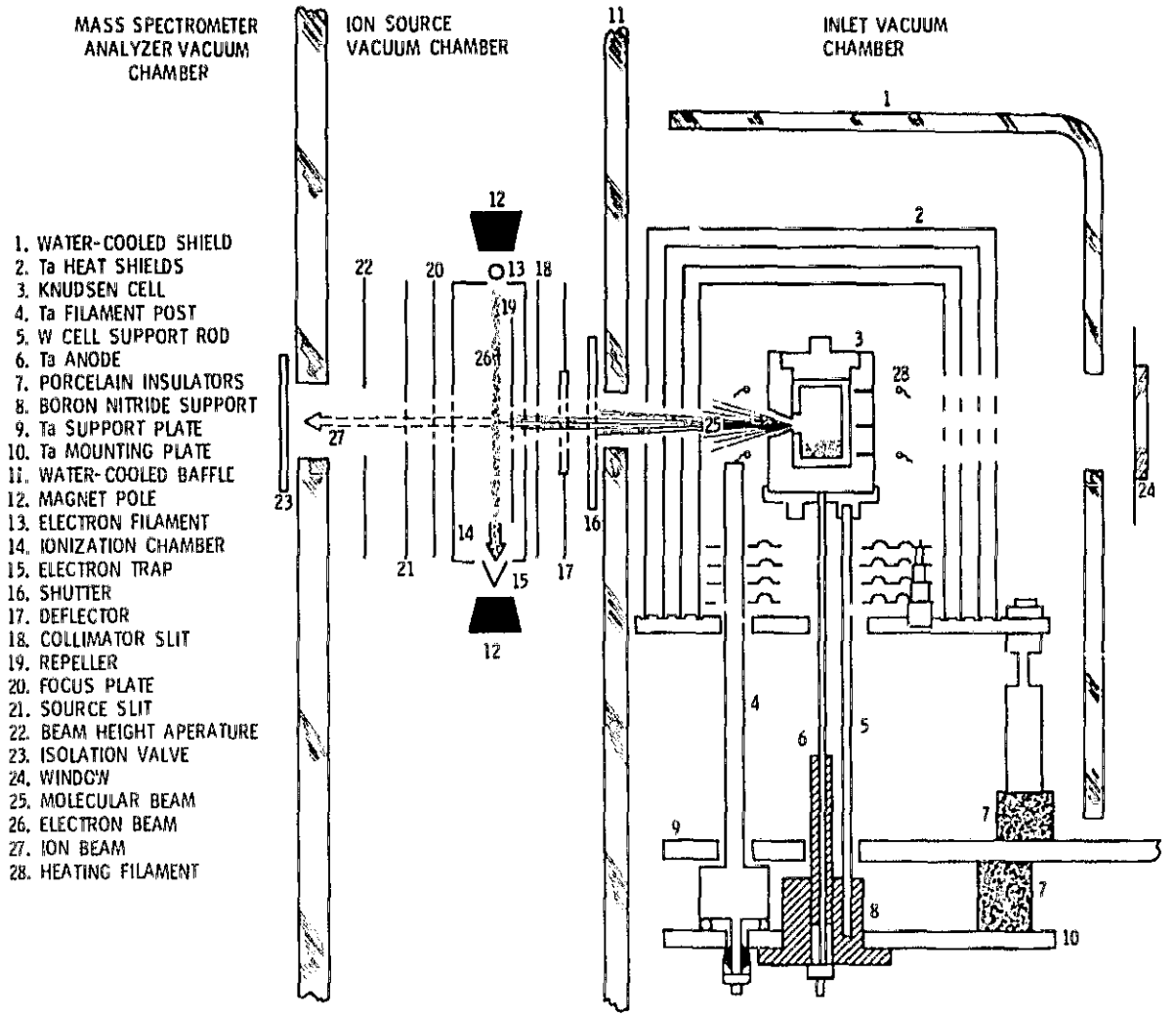

Figure 1. - Schematic of Knudsen cell oven assembly and ion source of mass spectrometer.

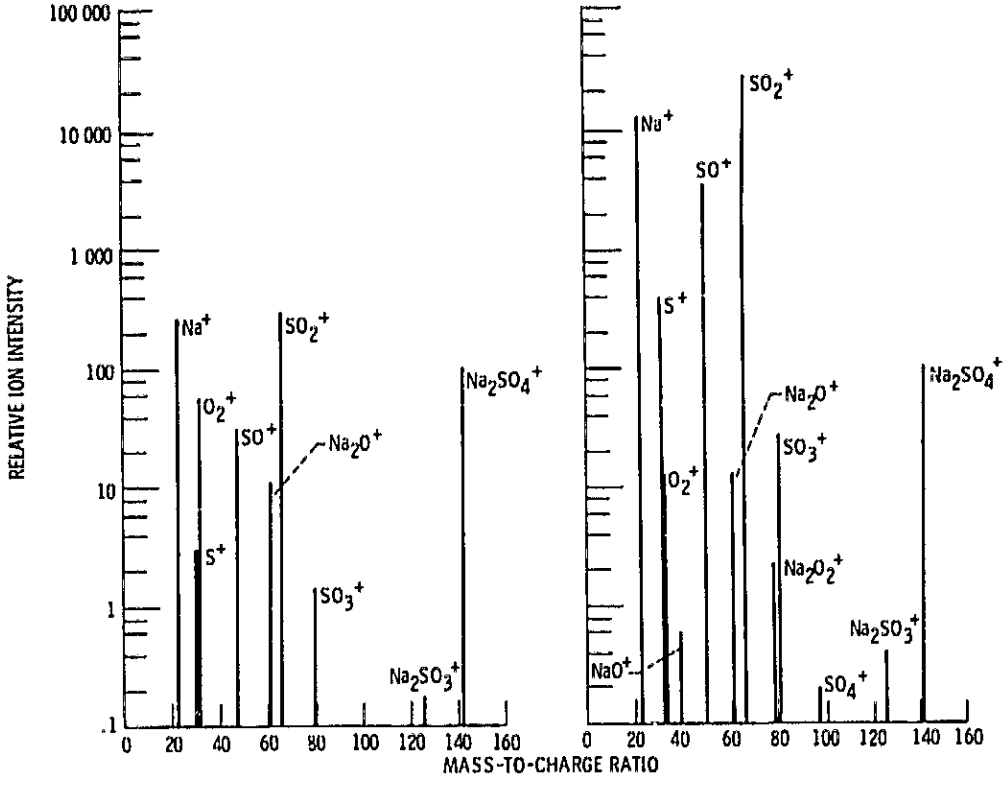

CS-71774 Figure 2. - Mass spectra of vapors over Na_2SO_4(l) at 30 electron volts ionizing energy.

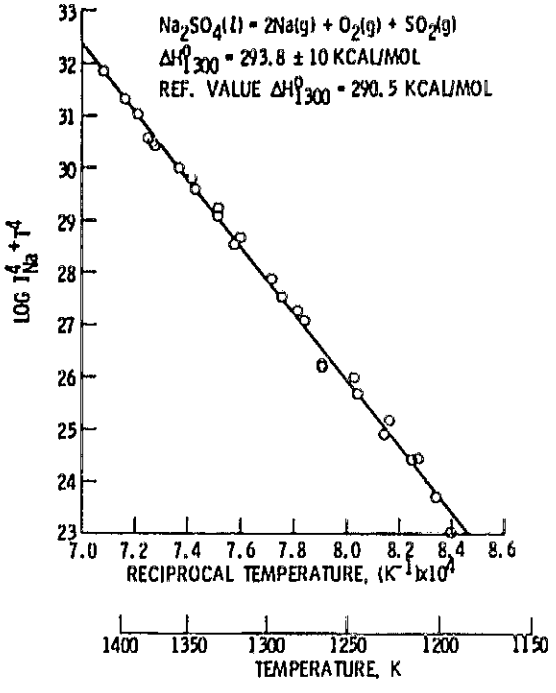

Figure 3. - Ion intensity versus reciprocal temperature for the $Na_2SO_4(l)$ decomposition reaction.

CS-71770

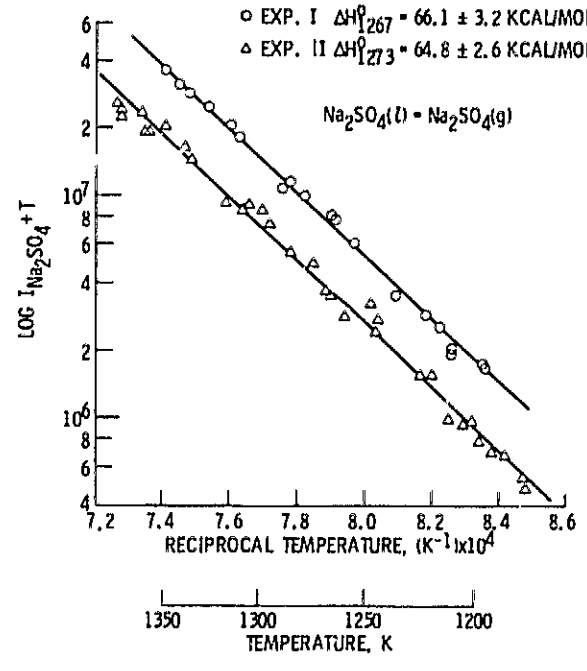

Figure 4. - Ion intensity versus reciprocal temperature for the $Na_2SO_4(l)$ vaporization reaction.

CS-71771

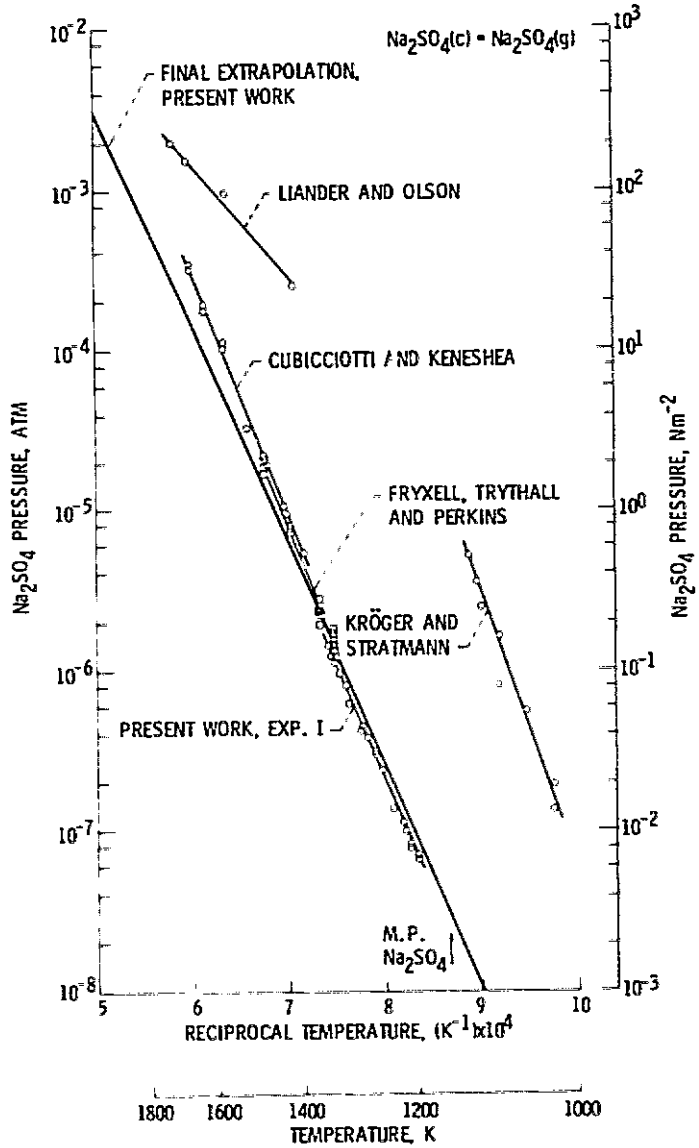

Figure 5. - Vapor pressure of sodium sulfate versus reciprocal temperature.

CS-71776

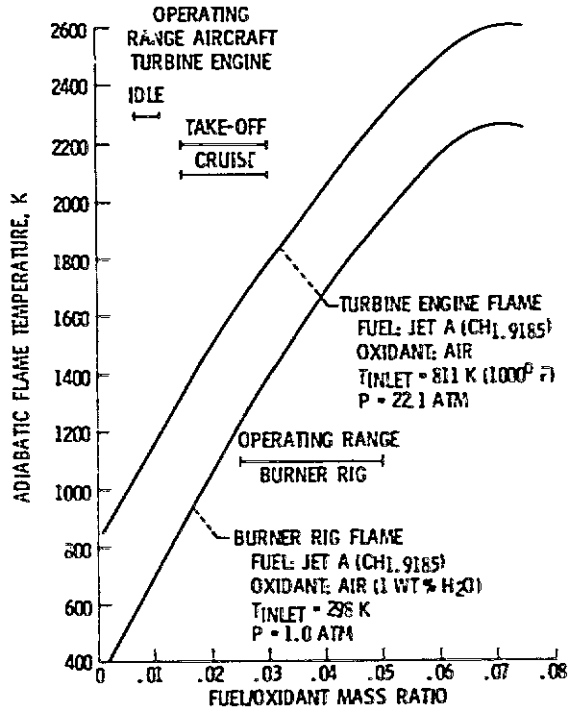

Figure 6. - Adiabatic flame temperature versus fuel/ oxidant mass ratio for turbine engine and burner rig flames.

CS-71772

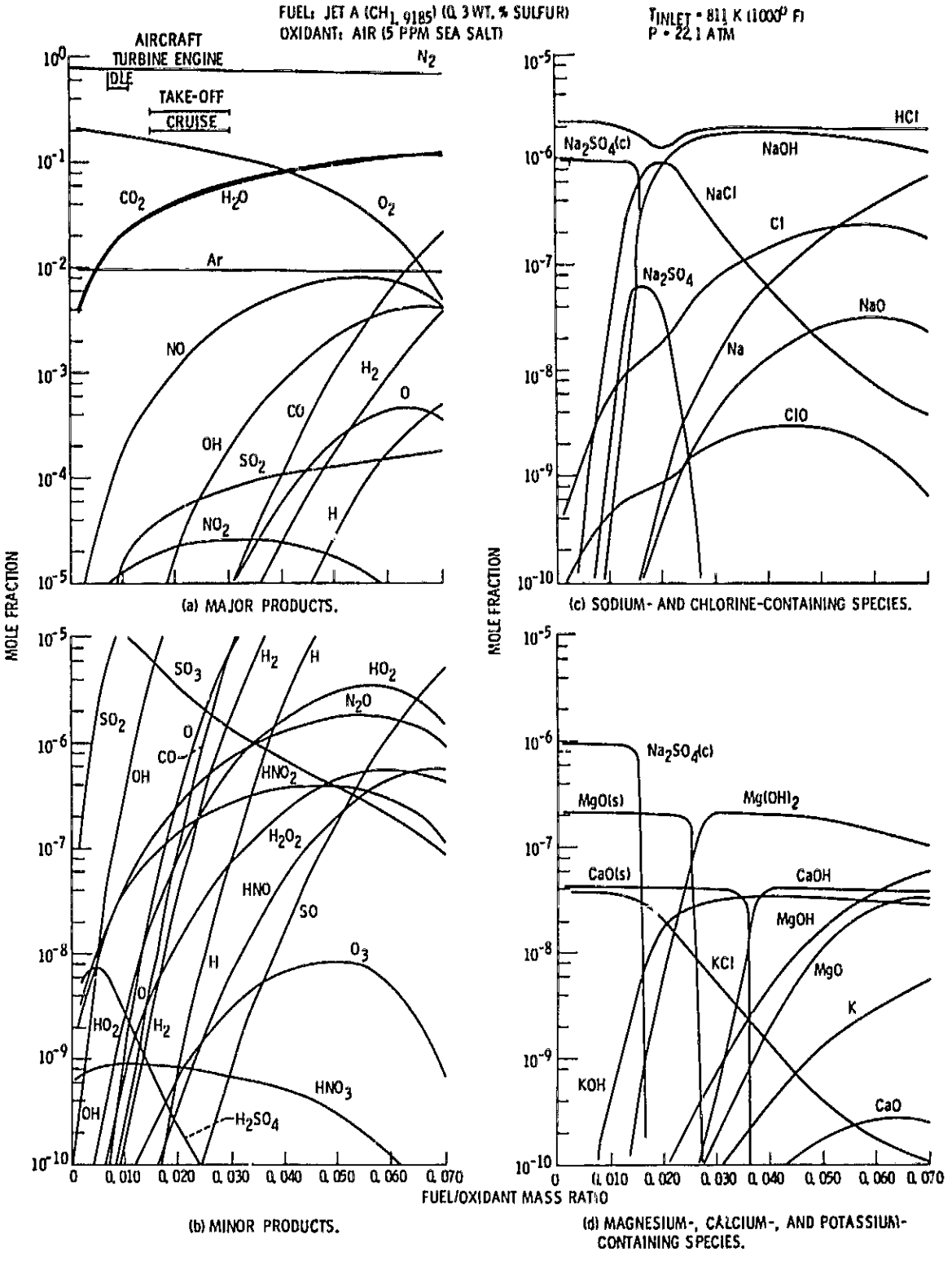

CS-71779

Figure 7. - Equilibrium chemical composition of flame gas versus fuel/oxidant mass ratio characteristic of an aircraft turbine engine with sulfur in the fuel and sea salt in the oxidant.

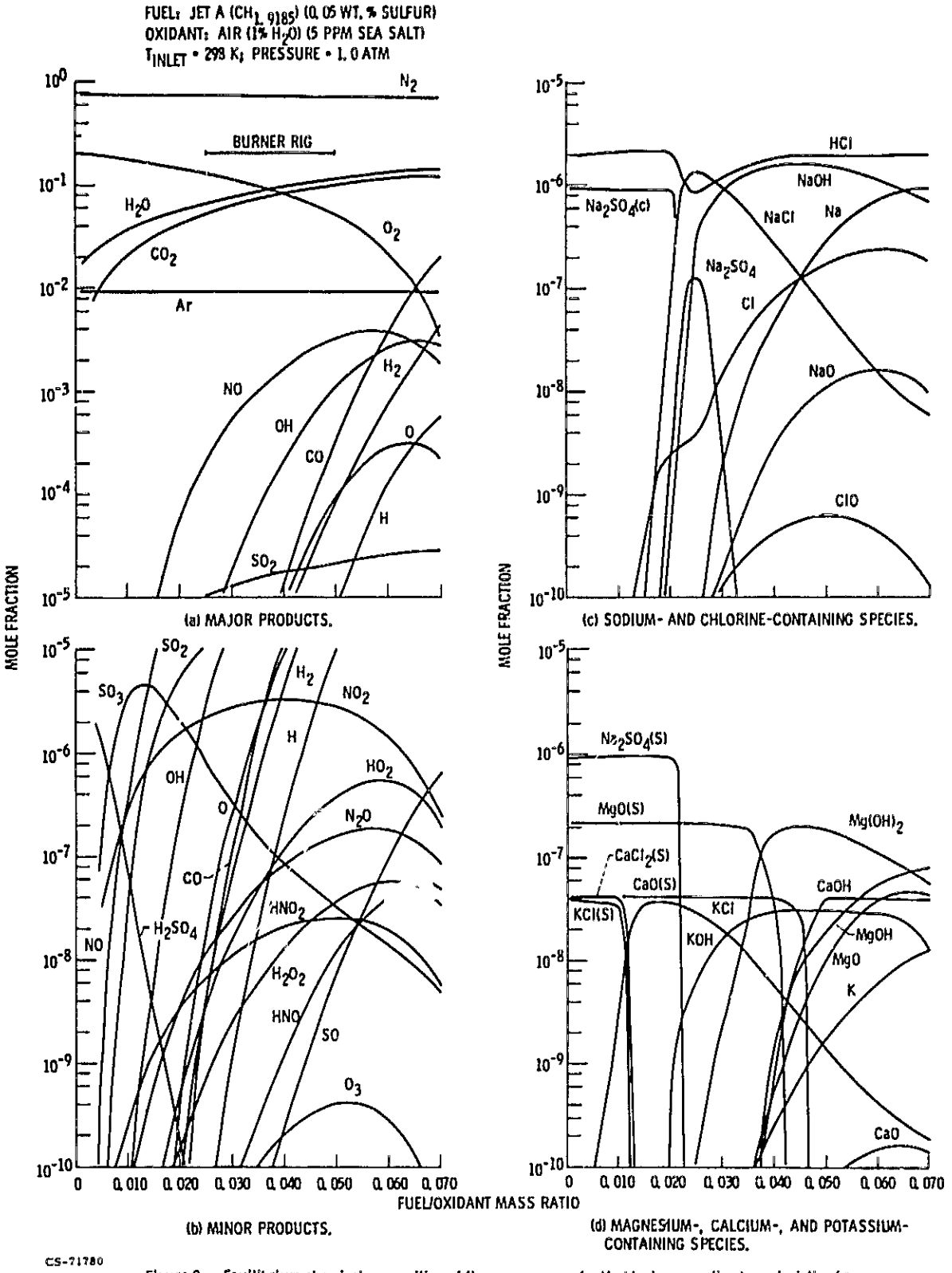

CS-71780

Figure 8. - Equilibrium chemical composition of flame gas versus fuel/oxidant mass ratio characteristic of an atmospheric burner rig with sulfur in the fuel and sea salt in the oxidant.

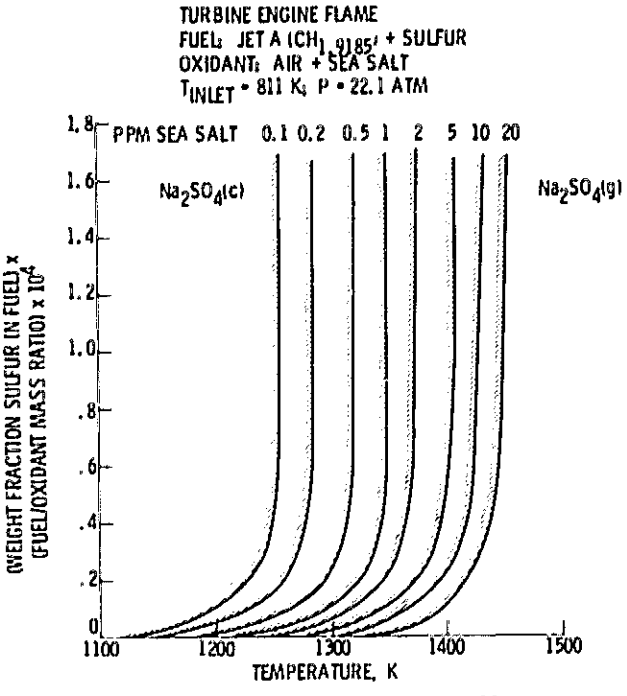

Figure 9. - Condensation temperature of Na_2SO_4 as a function of sulfur content and amount of fuel and sea salt concentration in oxidant for an aircraft turbine engine flame.

CS-71769

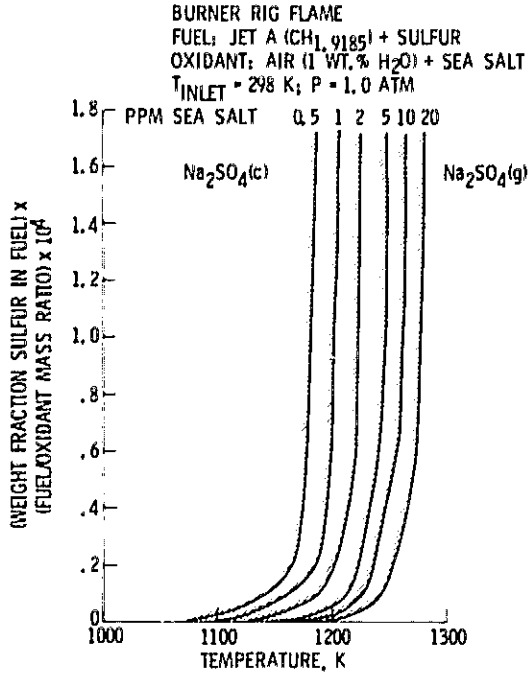

Figure 10. - Condensation temperature as a function of sulfur content and amount of fuel and sea salt concentration in oxidant for an atmospheric burner rig.

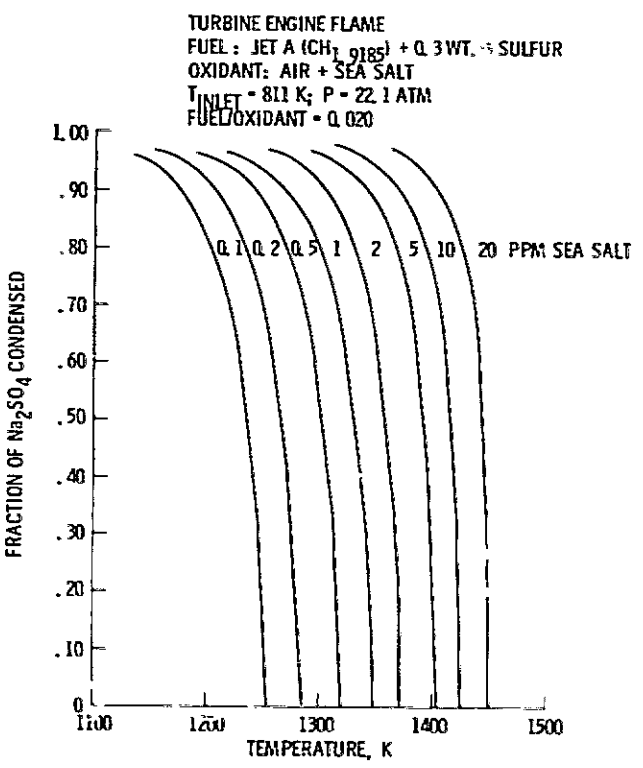

Figure 11. - Fraction of Na_2SO_4 condensed as a function of temperature and sea salt concentration for an aircraft turbine engine flame.

CS-71771

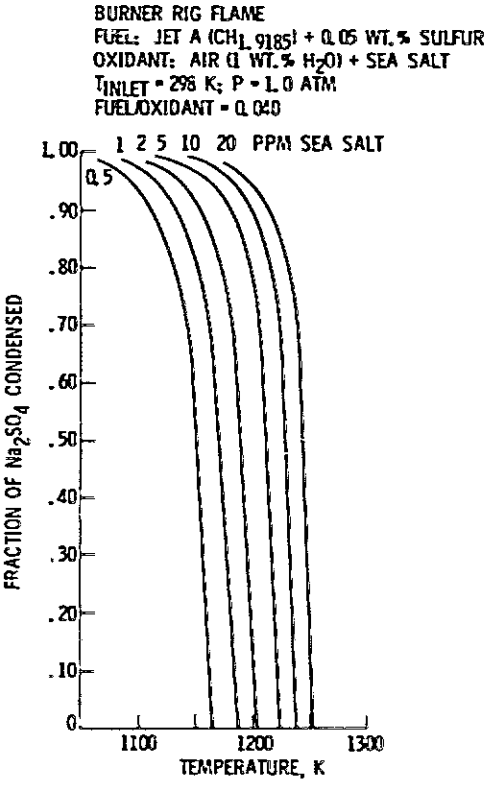

Figure 12. - Fraction of Na_2SO_4 condensed as a function of temperature and sea salt concentration for an atmospheric burner rig flame.